Smartphone Localization Inside a Moving Car for Prevention of Distracted Driving[1]

Gregory Johnson and Rajesh Rajamani[2]

Department of Mechanical Engineering

University of Minnesota

Abstract

This paper discusses a novel algorithm to automatically identify the position of a smartphone inside a moving vehicle, so as to detect whether it is being used by the driver or just a passenger of the car. This detection has applications to the prevention of distracted driving and can be used to automatically disable phone features such as texting when the phone is located in the driver's seat. The challenges in the smartphone localization problem come from the need to entirely use only accelerometers and gyroscopes already available on a typical phone, and the need to allow for any unknown 3-dimensional orientation of the phone while being carried by the driver or passenger of the car. First, the phone's real-time orientation is determined by identifying the vehicle's longitudinal and vertical axes in the phone reference frame. This provides the rotational matrix for conversion of accelerations and angular velocities measured on the phone to accelerations and angular velocities about the car axes. Next, the front-to-back pitching dynamics of the car during deceleration and the side-to-side roll dynamics during turning are characterized to detect whether the phone is in the driver's seat. The characterization of the roll and pitch dynamics are formalized using cross-covariances of sensor signals and a machine learning

[1] This project was supported in part by funding from the National Science Foundation, NSF Grant PFI-1631133.

[2] Email: rajamani@umn.edu

algorithm. Both simulations and extensive experiments are used to show that the developed system can accurately determine if the phone is being carried by the driver. The developed technology can be extremely useful for iPhones and other smartphones which can currently only detect whether the phone is on a moving car, but cannot detect whether it is being used by a driver or a passenger.

Keywords: Smartphone, phone location, distracted driving, smartphone sensors, support vector machine.

1. Introduction

Distracted driving from phone use is a major cause of vehicular accidents in the United States. The National Safety Council recently estimated that 26% of vehicular accidents involve phone usage or texting while driving [1], and recent research estimated that nearly half of teen drivers engaged in texting while driving [2]. This research also found that phone usage while driving was correlated with other risky driving behavior such as not wearing a seat belt and driving under the influence of alcohol. Thus, there is a clear need to discourage phone use while driving, and one approach to the problem is to automatically disable certain phone features (such as texting) while the user is actively driving. Automatic phone disabling requires the phone to first decide if it is in a moving vehicle and to second decide if it is in the driver seat position. The first decision is relatively straightforward based on GPS speed data, while the second decision concerning phone location inside the vehicle is more challenging.

Previous research has been published reporting methods to detect if the phone is in the driver's position [3]–[8]. Wang and colleagues [3] report a left/right localization method by comparing the

phone's accelerometer data to a reference accelerometer placed in the center of the vehicle (a small accessory plugged into the cigarette lighter port). Based on the measured centripetal acceleration during a turn, the system can determine if the phone is on the passenger or driver side of the reference, though no method is presented to differentiate between front and back. In [4], the authors use a very similar centripetal acceleration approach, but two phones are required, which must be carefully synchronized to within 100ms of each other. This requirement limits the practical application of such a system. Front and back position of the phone is determined by analyzing the signature pattern of road bumps on accelerometer data. An entirely different approach in [5] utilizes acoustic ranging to localize the phone inside the car by sending timed high frequency beeps from the car's audio system speakers. This approach requires a Bluetooth connection to the vehicle. Bo et al. [6] employed a machine learning approach to determine which side of the car the user enters and then use acceleration data during road bump events to determine if the phone is in the front or the rear. The authors also attempt to identify abnormal texting behavior (i.e. fast, intermittent typing may indicate texting while driving). The authors report an 87% recognition accuracy using a Naive Bayes classifier, though it is unclear how generalizable the algorithm is. Chu et al. [7] also use a machine learning approach, and train several support vector machines to recognize micro-motions related to driving, such as pressing the car pedal and entering the vehicle on the left hand side. The overall accuracy is 85%, but the approach fails depending on how the phone is carried, for instance by a woman in a purse.

The current generation Apple iPhone can detect when the user is in a moving car and will automatically turn off notifications. Patent filings assigned to Apple indicate that Apple has proposed to detect if the phone is being used by the driver based on a simple speed threshold and additional image processing from the phone's camera [8]. However, the phone's user may have

privacy concerns with granting camera access to the phone while driving.

Thus, none of the systems in literature provide a reliable system that only utilizes the sensors already on the smartphone. The most practical and ideal detection scheme of the phone's location inside the moving vehicle would have the following characteristics:

- The system should require no external hardware beyond the accelerometer, gyroscope and GPS sensors already available on the phone itself.
- The system should require no wireless connection to any other existing hardware on the vehicle, such as through Bluetooth.
- The system should require no special instrumentation of the car at all.

This paper will present a novel algorithm for determining the location of a smartphone inside a moving vehicle using only the motion signals from phone's three-axis gyroscope, accelerometer and GPS. This method relies on an understanding of the vehicle's pitch and roll dynamics [9]. As will be shown through simulation and experiments, when the car decelerates, the nose of the car will pitch downward, rotating about the vehicle pitch center. Thus, the front seat positions experience a downward motion while the rear seat positions experience an upward motion. The opposite is true while accelerating. Likewise, while turning, the vehicle tends to roll towards the outside of the turn about the roll center. While turning left, the left seat positions experience an upward motion, and the right seat positions experience a downward motion. The opposite is true during a right turn.

In combination, the pitch and roll dynamics offer the ability to uniquely identify seat position relative to the pitch and roll centers via motion signals recorded by the phone's IMU, in particular

the accelerometer and gyroscope. Once these signals are transformed into the vehicle's coordinate frame, features extracted in real-time from a moving window of motion data can be used for classification of the phone's location. This paper utilizes a linear support vector machine (SVM) to classify these features and identify if the phone is in the driver, the front passenger, the rear left passenger, or rear right passenger position. The feasibility of this approach is presented first through simulation and then through extensive experimental data.

Compared to previous research and available commercial technology, the main contributions of this paper are as follows:

1. The derivation of a method to identify seat position inside a moving vehicle based on the pitch and roll dynamics of a vehicle. Real-time data and knowledge of vehicle dynamics is exploited for the first time for this task in literature.
2. The development of a new method to transform the motion signals recorded in the phone's frame of reference to the vehicle's frame of reference.
3. The development of a completely self-contained system that only uses sensors already available on the phone.
4. Simulation and experimental demonstrations of the feasibility to classify the phone's seat position inside a moving vehicle using a machine learning algorithm based only on features extracted from a real-time moving window of motion data.

The remainder of this paper is organized as follows. In Section 2, the pitch and roll dynamics of a moving vehicle are presented. Section 3 presents a method to determine the orientation of the phone relative to the vehicle, necessary to transform the measured motion signals from the phone to the vehicle's coordinate frame of reference. Simulation studies are presented in Section 4,

followed by experimental results in Section 5. Finally, seat position classification using a linear support vector machine is presented in Section 6.

2. Vehicle Dynamic Model

The classification algorithm developed in this paper relies on the pitch and roll dynamic behaviors of the vehicle [9]. Half car models for pitch and roll dynamics for preliminary simulation evaluations are presented in this section. The coordinate system for the car is defined as forward longitudinal ($+x$), left lateral ($+y$), and up vertical($+z$). The rotational angles are roll ϕ about the x axis and pitch θ about the y axis.

The free body diagram for the vehicle roll model is shown in Fig. 1. Here, the vehicle rotates about the roll center due to the lateral acceleration caused by turning and by lateral translation. The suspension force is modeled as a linear spring and damper with deflection $z(t) = \left(\frac{\ell_w}{2}\right) sin(\phi)$, spring constant k, and damping coefficient b as follows:

$$F_S(t) = k\left(\frac{\ell_w}{2}\right) sin(\phi) + b\left(\frac{\ell_w}{2}\right)\dot{\phi} cos(\phi) \quad (1)$$

where F_S is the suspension force, ϕ is the roll angle, ℓ_w is the track width of the vehicle, k is the suspension stiffness and b is the damping coefficient.

The lateral acceleration is treated as a force input at the center of gravity (CG) in the moment balance equation taken about the roll center. This couples the roll dynamics to the lateral dynamics through the lateral acceleration a_y term:

$$(I_{\mathrm{xx}} + mh^2)\ddot{\phi} = ma_y h cos(\phi) + mghsin(\phi) - k\left(\frac{\ell_w^2}{2}\right) sin(\phi) - b\left(\frac{\ell_w^2}{2}\right)\dot{\phi}cos(\phi) \qquad (2)$$

where $(I_{xx} + mh^2)$ is the moment of inertia taken at the roll center, h is the distance from the roll center to the CG, m is the vehicle mass and g is the gravitational constant. More detailed simulation models for roll dynamics can be found in other papers from this journal, such as [14], [15] and [16]. However, the model presented here is adequate for the roll dynamics in order to evaluate in simulations how the lateral motion and acceleration of the car cause roll and how these signals influence the accelerometer and gyroscope signals read by the sensors on the phone. Extensive experimental evaluations of the developed algorithm using measurements on real car maneuvers will later be presented to serve as a more reliable indicator of the developed algorithm's effective performance.

A similar equation results for the vehicle pitch dynamics if the variables in (1) and (2) are redefined according to Fig. 2 with the appropriate substitutions of I_{yy} for I_{xx} and the longitudinal acceleration a_x for a_y. In this case, the equation relating the pitch dynamics to the longitudinal acceleration and deceleration is given by

$$(I_{yy} + mh^2)\ddot{\theta} = ma_x h cos(\theta) + mghsin(\theta) - k\left(\frac{\ell_f^2+\ell_r^2}{2}\right) sin(\theta) - b\left(\frac{\ell_f^2+\ell_r^2}{2}\right)\dot{\theta}cos(\theta) \qquad (3)$$

where, θ is the pitch angle, $\left(I_{yy} + mh^2\right)$ is the moment of inertia taken at the pitch center, h is the height from the pitch center to the CG, m is the vehicle mass, k is the suspension stiffness, b is the damping coefficient, ℓ_f is the distance from the CG to the front tires, ℓ_r is the distance from the CG to the rear tires and g is the gravitational constant.

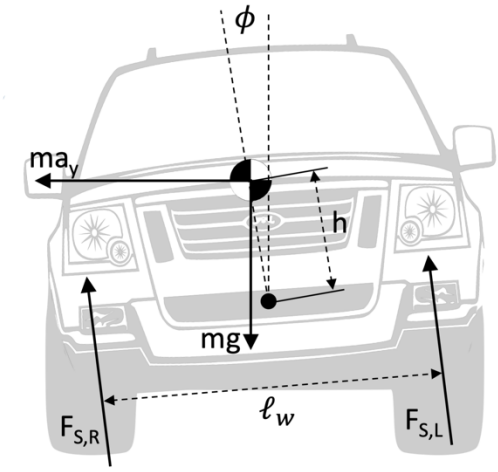

Fig. 1. Free body diagram for vehicle roll.

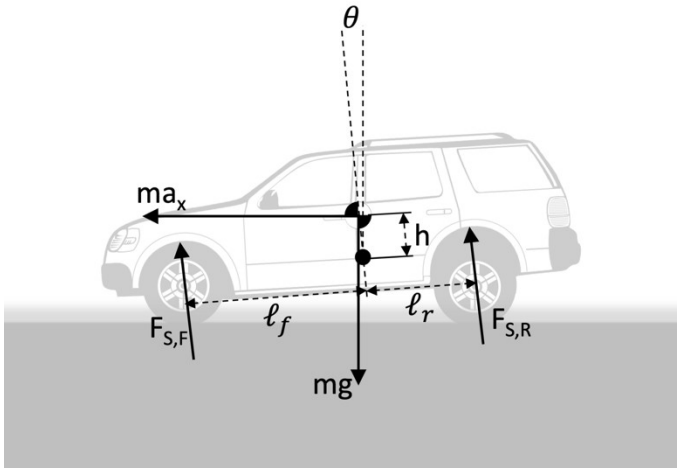

Fig. 2. Free body diagram for vehicle pitch

3. Real-Time Estimation of Phone to Vehicle Orientation

The smartphone user may carry the phone in his/her pocket, in a purse, on a display stand in the car or they may be holding it in their hands. Thus the orientation of the phone with respect to the car can be completely arbitrary and all three Euler angles of rotation can be unknown. Since the motion signals recorded by the phone must be transformed from the phone coordinate frame to the vehicle coordinate frame, real-time knowledge of the orientation of the phone relative to the

vehicle is required.

There are several possible approaches to finding the orientation of the phone, two of which are presented next, and their relative advantages and limitations discussed. Please note that orientation can be parameterized a number of ways, the three primary methods being Euler angles, quaternions, or the 3x3 direction cosine matrix (DCM). A complete discussion of the merits and drawbacks of these three parameterizations is outside the scope of this paper, but the DCM (also known as the rotation matrix) is used here, mainly because it avoids singularity issues of other parameterizations. A full treatment of orientation parameterizations may be found in [10].

One potential method to estimate the phone orientation relative to the car is to first estimate the orientation of the phone relative to earth, and then the orientation of the vehicle relative to earth. Call these orientation DCMs (or rotation matrices) R_{earth}^{phone} and R_{earth}^{car}, respectively, where R_a^b refers to the DCM between frames a and b. Once these are known, the orientation of the phone relative to the car can be determined as:

$$R_{car}^{phone} = (R_{earth}^{car})^T R_{earth}^{phone} \tag{4}$$

R_{earth}^{car} is relatively straightforward to estimate using GPS course information available on the phone, which reports the direction of travel of the vehicle. A typical method to estimate R_{earth}^{phone} would be to utilize measurements of two known inertial directions, such as the gravity vector with the accelerometer and earth's magnetic field, which is locally a constant vector, with the magnetometer. These can then be optimally fused with gyroscope measurements using, for instance, a Kalman Filter. The main problem with this approach is that the presence of unknown magnetic disturbances, such as steel components in the car, can badly corrupt the magnetic

measurement.

Here, a simpler approach is used to directly determine R_{car}^{phone} without needing to transform to the earth frame first. At any given time, the accelerometer measurement is the vector sum of gravity and the vehicle acceleration:

$$\vec{a}_{measured} = \vec{a}_{gravity} + \vec{a}_{vehicle} \tag{5}$$

While braking, the dominant components of the measured acceleration will be gravity plus the longitudinal deceleration of the vehicle, with smaller components being road vibrations and the roll/pitch transient dynamics. Thus, while braking, the measurement can be approximated as:

$$\vec{a}_{measured} = \vec{a}_{gravity} + \vec{a}_{longitudinal} \tag{6}$$

While stopped (as determined by GPS) or by averaging acceleration data over a long period of time, a good measurement of $\vec{a}_{gravity}$ is available. This can then be subtracted from the total measured acceleration during a brake maneuver to determine the longitudinal acceleration. Thus, the gravity measurement gives the direction of the vehicle z-axis, while the longitudinal acceleration during braking gives the vehicle x-axis. From these, R_{car}^{phone} can be estimated using a static attitude determination algorithm such as TRIAD [10], presented next.

Let $\{v_1, v_2, v_3\}$ be the representation of an orthonormal set of vectors in the vehicle's frame, and let the representation of these same vectors in the phone's frame be denoted as $\{p_1, p_2, p_3\}$. Since R_{car}^{phone} is the rotation matrix that defines the orientation of the phone to the car, then:

$$R_{car}^{phone} = [p_1 \quad p_2 \quad p_3][v_1 \quad v_2 \quad v_3]^T \tag{7}$$

It is assumed that the terrain is flat, i.e. there is no significant road gradient. Let $r_{g,c} = [0 \quad 0 \quad -1]^T$ represent the gravity vector in the vehicle frame and $r_{g,p}$ represent a measurement of the gravity vector in the phone frame. Likewise, let $r_{x,c} = [1 \quad 0 \quad 0]^T$ represent the longitudinal axis of the vehicle and $r_{x,p}$ be a measurement of the vehicle's longitudinal direction in the phone's frame obtained during a braking maneuver, as explained above. R_{car}^{phone} can now be determined from (7) by creating the following sets of orthonormal reference and body vectors:

$$v_1 = r_{g,c} \quad , \quad v_2 = \frac{v_1 \times r_{x,c}}{\|v_1 \times r_{x,c}\|} \quad \text{and} \quad v_3 = v_2 \times v_1 \tag{8}$$

$$p_1 = \frac{r_{g,p}}{\|r_{g,p}\|} \quad , \quad v_2 = \frac{p_1 \times r_{x,p}}{\|p_1 \times r_{x,p}\|} \quad \text{and} \quad p_3 = p_2 \times p_1 \tag{9}$$

Experimental Verification:

To demonstrate the use of the above method, accelerometer and gyroscope data from a smartphone was collected at 100Hz during normal driving with the phone in three different orientations, as shown in Fig. 3.

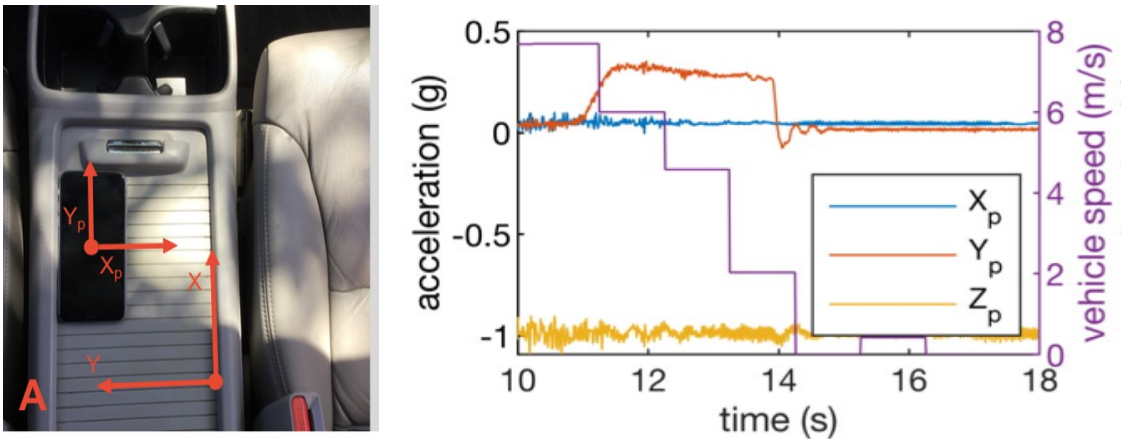

(a) Experimental data with phone oriented in the forward longitudinal direction

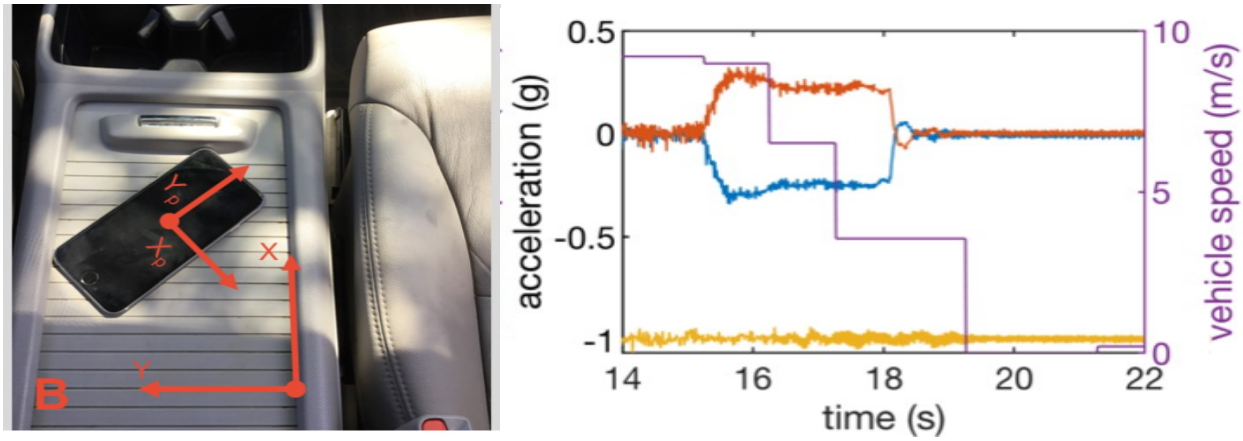

(b) Experimental data with phone oriented obliquely in the horizontal plane

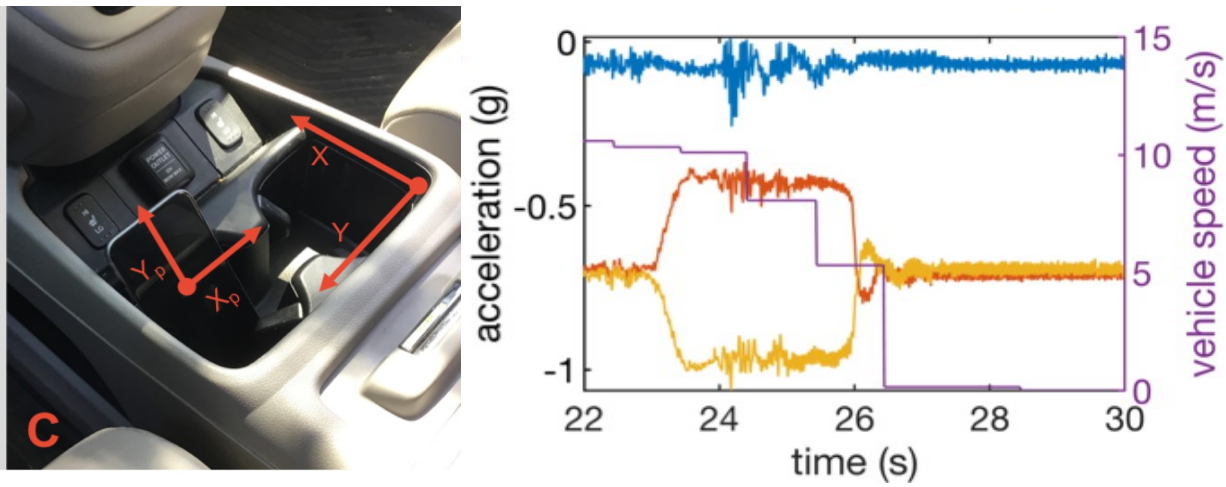

(c) Experimental data with phone oriented at an approximate 45-degree vertical angle in 3-dimensional space

Fig. 3. Three experiments to demonstrate the phone orientation estimation procedure using the measured acceleration during braking events as a reference for the vehicle longitudinal axis. The event can be detected as braking by the decrease in speed, available from the phone's GPS data (purple line in the data plots).

TABLE I

EXAMPLE DCM ESTIMATES FOR THREE PHONE ORIENTATIONS

ID	$r_{g,p}$	$r_{x,p}$	R_{car}^{phone} (experimental)	R_{car}^{phone} (expected)
A	$\begin{bmatrix} 0.04 \\ 0.02 \\ -0.99 \end{bmatrix}$	$\begin{bmatrix} 0.00 \\ 0.30 \\ 0.00 \end{bmatrix}$	$\begin{bmatrix} 0.02 & 1.00 & 0.02 \\ -1.00 & 0.02 & -0.05 \\ -0.05 & -0.02 & 1.00 \end{bmatrix}$	$\begin{bmatrix} 0.0 & 1.00 & 0.0 \\ -1.00 & 0.0 & 0.0 \\ 0.0 & 0.0 & 1.00 \end{bmatrix}$
B	$\begin{bmatrix} 0.00 \\ 0.00 \\ -1.00 \end{bmatrix}$	$\begin{bmatrix} -0.24 \\ 0.22 \\ 0.00 \end{bmatrix}$	$\begin{bmatrix} -0.74 & 0.67 & 0.00 \\ -0.67 & -0.74 & 0.00 \\ 0.00 & 0.00 & 1.00 \end{bmatrix}$	$\begin{bmatrix} -0.707 & 0.707 & 0.00 \\ -0.707 & -0.707 & 0.00 \\ 0.00 & 0.00 & 1.00 \end{bmatrix}$
C	$\begin{bmatrix} -0.07 \\ -0.71 \\ -0.70 \end{bmatrix}$	$\begin{bmatrix} 0.01 \\ 0.28 \\ -0.28 \end{bmatrix}$	$\begin{bmatrix} -0.03 & 0.70 & -0.71 \\ -1.00 & 0.03 & 0.07 \\ 0.07 & 0.71 & 0.70 \end{bmatrix}$	$\begin{bmatrix} 0.0 & 0.707 & -0.707 \\ -1.00 & 0.0 & 0.0 \\ 0.0 & 0.707 & 0.707 \end{bmatrix}$

In Fig. 3A, the orientation of the phone relative to the car was visually aligned such that the phone's y-axis was aligned with the vehicle's x-axis, and the phone's z-axis was vertical. The vector $r_{g,p} = [0.04 \quad 0.02 \quad -0.99]^T$ was determined by taking the mean accelerometer measurement when the vehicle speed measurement was 0. The vector $r_{x,p} = [0.0 \quad 0.30 \quad 0.00]^T$ was determined by subtracting $r_{g,p}$ from the mean accelerometer measurement during the brake maneuver at 12s. Equation (7) gives a very reasonable estimate of the phone orientation as:

$$R_{car}^{phone} = \begin{bmatrix} 0.02 & 1.00 & 0.02 \\ -1.00 & 0.02 & -0.05 \\ -0.05 & -0.02 & 1.00 \end{bmatrix} \tag{9}$$

The above approach to estimating the phone orientation was repeated on two additional orientations, shown in Fig. 3 (b) and Fig. 3 (c) with results summarized in Table I. In experiment B, the phone was placed horizontal with the display up on the center console, rotated 135 degrees clockwise about the vertical axis, as measured with a 45-degree triangle referenced against the vehicle console surface. In experiment C, the phone was placed in the vehicle cup holder at a vertical angle of 45 degrees, measured with an inclinometer application on the phone. The +x axis of the phone was visually oriented with the -y axis of the vehicle. As seen from a comparison of the third and fourth columns of Table I, in all three experiments, the method provides very good estimates of the phone orientation relative to the vehicle. It should be noted that the small differences between the entries in columns 3 and 4 are likely due to the phone not exactly being at 45° orientations in case B and case C, since these orientations were only done visually or approximately.

4. Simulation Studies

The objective of this section is to evaluate the pitch angular velocity and vertical acceleration responses of the vehicle during braking and the roll angular velocity and vertical accelerations during turning. The nature of these responses, as measured by the sensors on the smartphone, will depend on the location of the phone inside the car. As we shall see, the nature of these responses can serve as a reliable indicator of the phone location and whether it is located in the driver seat of the car.

Fig. 4 shows the simulation response of the car to a series of step changes in longitudinal acceleration. At $t = 1s$, the brakes and a longitudinal deceleration of $0.4g$ are applied until $t = 5s$. At $t = 8s$, an acceleration of $0.4g$ is applied until $t = 12s$. The top part of Fig. 4 shows the vertical acceleration and the pitch angular rate at the front seats of the car. The bottom part of Fig. 4 shows the vertical acceleration and the pitch rate at the rear seats of the car. The step response shows an underdamped oscillatory behavior in both sensor signals. Clearly, the vertical accelerations in the front and back are equal but opposite in direction. On the other hand, the pitch angular rate (as measured by a gyroscope) is the same in both the front and rear seats of the car

during braking/ acceleration.

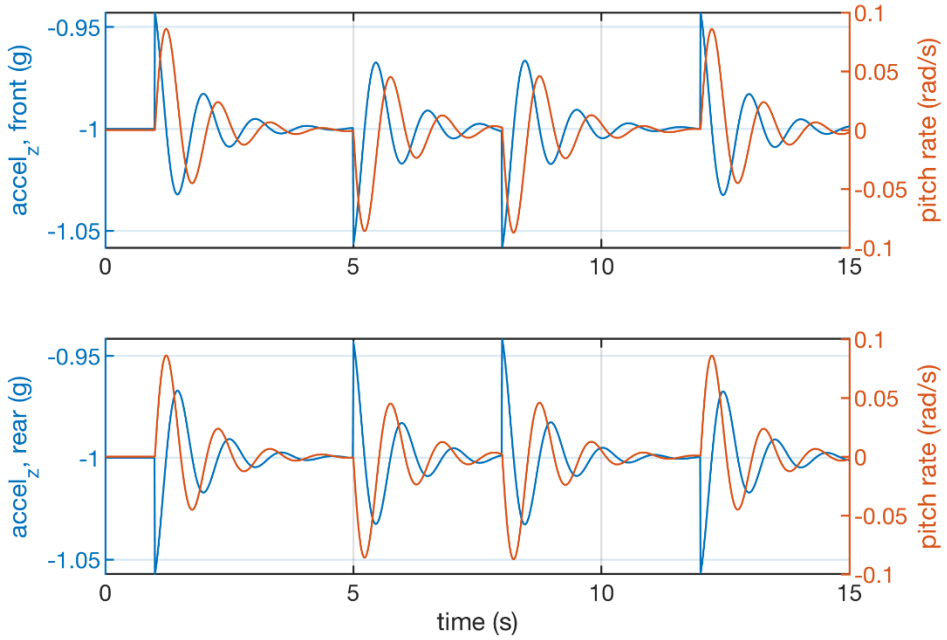

Fig. 4: Simulated response to several step changes in longitudinal acceleration. At t=1s, the brakes and a longitudinal deceleration of 0.4g are applied until t=5s. At t=8s, an acceleration of 0.4g is applied until t=12s. The top plot shows the pitch rate and the vertical acceleration for the front seats, and the bottom plot shows the pitch rate and the vertical acceleration for the rear seats.

In order to capture the differences in the vertical acceleration behavior at the front and back seats, integrating the vertical acceleration twice shows the rear vertical position is positive when the pitch angle is positive, and the opposite behavior for the front vertical position. This suggests a useful feature for front/back classification would be the correlation of the vertical-axis accelerometer data integrated twice with the pitch-axis gyroscope data integrated once during periods with longitudinal acceleration, as summarized in Table II below. Likewise, a useful feature for left/right classification would be the correlation of the vertical-axis accelerometer data integrated twice with the roll-axis gyroscope data integrated once during a turn. However,

integrating accelerometer signals twice and gyroscope signals once is non-trivial due to the presence of bias errors in the sensor signals. These bias errors are inevitable and time-varying so that they will always exist and cannot be compensated fully. Careful high and low pass filtering could solve some of these bias and integration-drift issues, but nonetheless, trying to experimentally calculate vertical displacements and comparing to pitch and roll angles is not an easy approach.

TABLE II

RELATIONSHIPS BETWEEN PITCH AND ROLL ANGLES VS. VERTICAL DISPLACEMENT.

Position	a_x	$\phi_{pitch} = \int g_y$	$z = \iint a_z$
Front	> 0 (accelerating)	< 0	> 0
	< 0 (braking)	> 0	< 0
Rear	> 0	< 0	< 0
	< 0	> 0	> 0
Position	a_y	$\phi_{roll} = \int g_x$	$z = \iint a_z$
Left	> 0 (left turn)	> 0	> 0
	< 0 (right turn)	< 0	< 0
Right	> 0	> 0	< 0
	< 0	< 0	> 0

A more desirable approach is to find classification features in the accelerometer and gyroscope signals that don't require integration at all. Careful inspection again of the data in Fig. 4 shows that the oscillatory responses for front and back acceleration are 180-degrees out of phase. Further, when comparing the acceleration responses to the pitch rate at each location, it is clear that there is a phase lag between these signals and the phase lag is different at the front and rear seats of the car. This phase lag could therefore be a useful classification feature. Hence, the signal cross covariance between these two sensor signals is utilized, in which the signal means are subtracted from two signals and the cross correlation is calculated as follows [11]:

$$c_{xy} = \begin{cases} \sum_{n=0}^{N-m-1}(x_{n+m} - \bar{x})(y_n - \bar{y}), & m \geq 0 \\ c_{xy}(-m), & m < 0 \end{cases} \tag{10}$$

where x is the first sensor signal (from the accelerometer), y is the second sensor signal (from the gyroscope) and m is the size of the lag, in terms of number of samples, which is being used to calculate the cross-correlation.

The cross covariances between vertical acceleration and pitch-axis angular rate are shown in Fig. 5 for the simulation data of Fig. 4, for a range of lag values. It can be seen that the cross-covariance decreases with time lag for the sensor signals on the front seats of the car. On the other hand, the cross-covariance increases with time lag for the sensor signals in the rear seats of the car. The clear difference between the cross covariances for front and rear and their different behavior with time lag suggest that this could be a useful classification feature that can be reliably used to detect phone location. The same signal-processing approach can also be exploited with the roll gyroscope signal and vertical accelerometer signal to determine location being on the left or right side of the car. This simulation section has suggested a signal-processing approach for front-back

and right-left classification of the phone location. In the following section, this signal-processing approach is applied to experimental data and its performance in a number of experimental car maneuvers is evaluated.

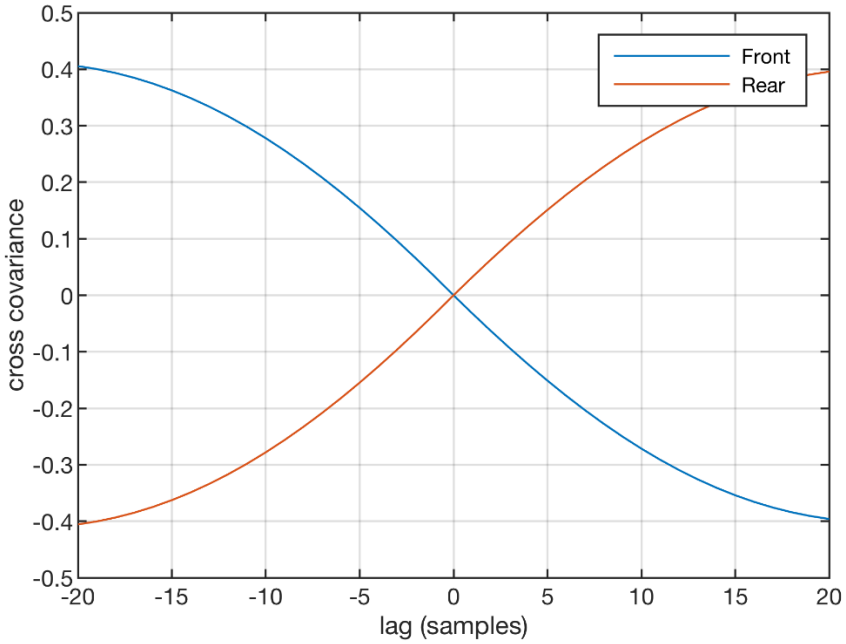

Fig. 5: Cross covariance of vertical acceleration to pitch-axis angular rate of simulated data.

5. Experimental Results

Experiments are performed to verify whether the cross-covariance between the vertical accelerometer and the pitch or roll gyroscope signals can reliably identify the location of the smartphone in the car. In particular, the cross-covariance with the pitch gyroscope and its variation with time lag is used to identify whether the phone is in the front or rear seats of the car. The cross-covariance with the roll gyroscope and its variation with time lag is used to identify whether the phone is in the left or right sides of the car.

A smartphone (Apple iPhone 6S) was used to collect data in a car while being used at different

seat locations in the car. A sampling rate of 100 Hz was used and the data collected was entirely from the sensors only on the phone. The driving took place alongside normal day time traffic on urban roads and the speeds varied but were kept to less than 35 mph (16 m/s).

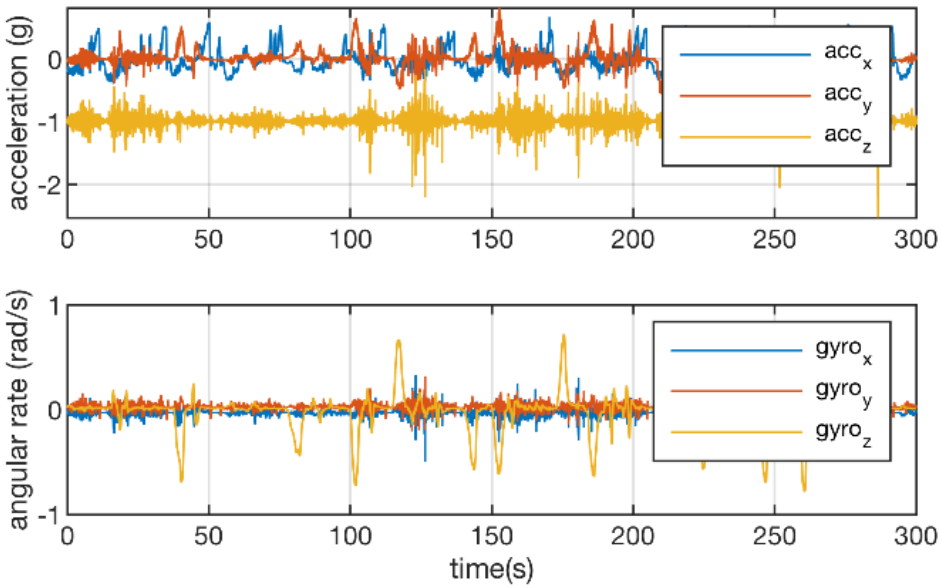

Fig. 6: Example raw accelerometer and gyroscope data taken during city street driving for back right passenger.

The phone was placed in each of four positions (driver, front passenger, back left passenger, back right passenger) for two data sets of 5 minutes each for all four seat positions. Thus a total of 40 minutes of data was obtained. To keep the phone from shifting, it was secured to the vehicle carpet using hook and loop strap. For the front seat positions, the phone was secured to the vehicle carpet approximately under the driver's left or front passenger's right knee, thus midway between the dash and the front seat in the longitudinal direction. For the rear seat positions, the phone was secured to the vehicle carpet where the back of the seat attaches to the vehicle frame, roughly approximating the left pants pocket position of the left rear passenger and right pants pocket of the right rear passenger. An example section of data is shown in Fig. 6. Zoomed in sections of experimental data are shown in Fig. 7 for front and rear positions while braking and in Fig. 8 for

left and right positions while turning. For the pitching oscillations near 2.5 Hz in Fig. 7, the phase difference between the pitch-axis angular rate and vertical acceleration is clearly evident. As expected, the two signals have a phase difference of 90 degrees, while the sign of the accelerometer is opposite when comparing front to rear seat positions. For a 2.5 Hz oscillation, a 90 degree phase difference suggests the cross covariances should have a peak or valley near a lag of 10 samples for a 100 Hz sampling frequency.

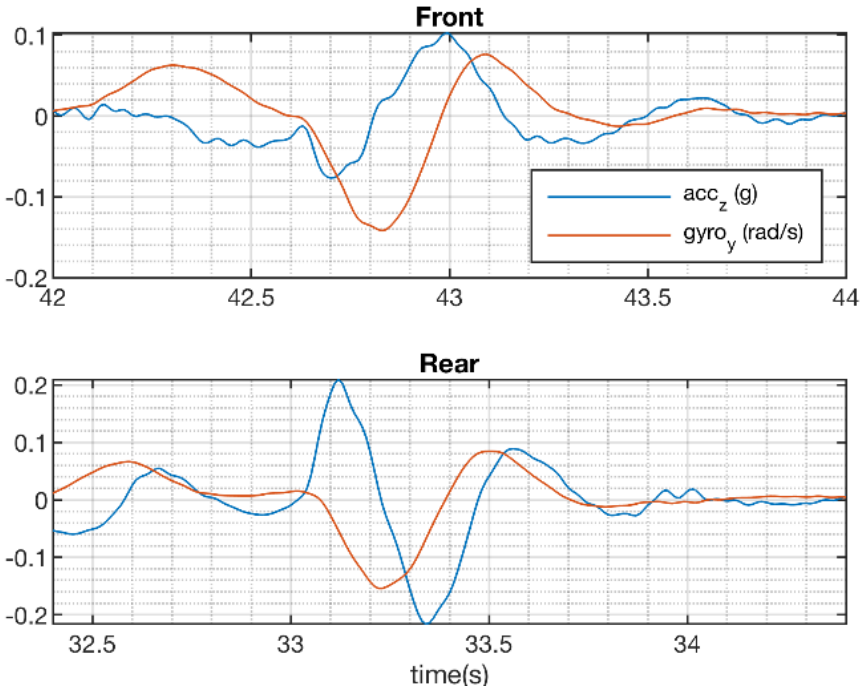

Fig. 7: Example accelerometer and gyroscope data taken during city street driving for front and rear positions, with gravity removed from the accelerometer signal. The signals are from two different braking events at the moment the vehicle comes to a complete stop and returns to a horizontal position. The 90 degree phase difference between the pitch axis gyroscope and vertical accelerometer signals is evident, while the accelerometer signal has the opposite sign comparing front to rear.

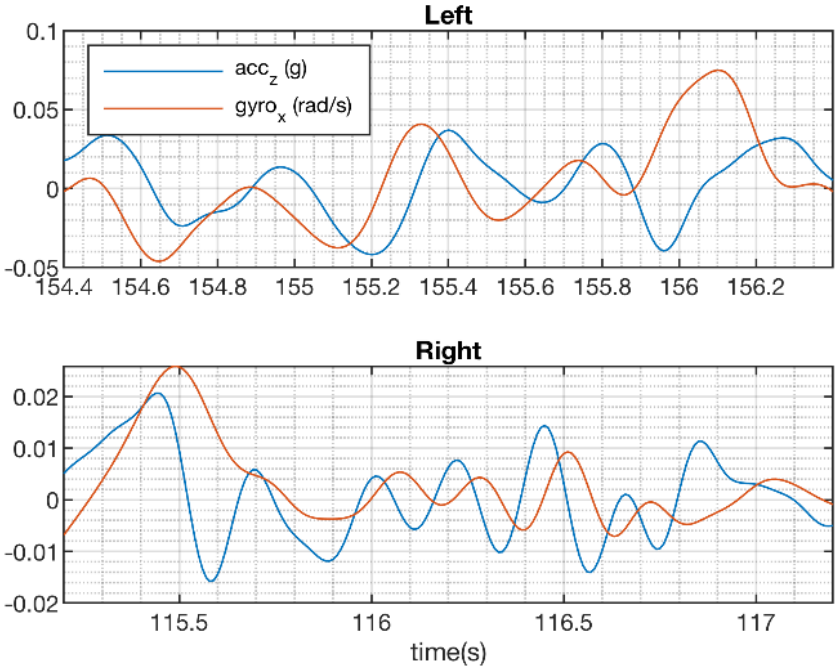

Fig. 8.: Example vertical accelerometer and roll axis gyroscope data taken during city street driving for left and right positions, with gravity removed from the accelerometer signal. The signals are from two different turning events. The 90 degree phase difference between roll axis gyroscope and vertical accelerometer signals is evident, while the accelerometer signal has opposite sign comparing left to right.

The cross covariances for vertical acceleration to pitch-axis angular velocity and vertical acceleration to roll-axis angular velocity are shown in Fig. 9 for a five minute data set of each seat position. The raw data was first low pass filtered prior to computing the cross covariances. Fig. 9 clearly shows that each seat position has a unique combination of cross covariances. As expected, the cross covariances have peaks and valleys near a lag of 10 samples. The experimental data follows the same overall behavior as the simulated cross covariances in Fig. 5. This indicates that the cross covariance is a good choice as a classification feature.

After experimental verification of the basic behavior of cross-covariance of the accelerometer-gyroscope pairs with phone location inside the car, a systematic algorithm for automatically

detecting phone location is developed in the next section.

6. Experimental Results on Automatic Phone Location Identification using a Support Vector Machine

The experimental results of the previous section verified that there is a clear and reliable relationship between phone location and the cross-covariance of accelerometer-gyroscope paired data. The next step is to develop and implement an automatic location identification algorithm that makes use of these cross-covariances. This section develops a machine learning algorithm consisting of a support vector machine for performing this automatic location identification.

Fig. 9 shows cross-covariances of experimental data for the 4 different locations of the phone. In each set of data, the cross-covariances between pitch gyroscope and vertical accelerometer and between roll gyroscope and vertical accelerometer are shown. In each data set 5 minutes of driving data is used. It can be seen that the slopes of the two cross-covariances are unique in the 4 different phone locations. For example, in the driver seat location, the pitch gyroscope cross-covariance has a negative slope while the roll gyroscope cross-covariance has a positive slope around the zero lag point. Likewise, there is a unique combination of positive and negative slopes for the 4 different locations.

Ideally, the phone should recognize its location inside the vehicle in a much shorter period than 5 minutes, so the same data was divided up into shorter 45 second long sections, overlapping by 15 seconds. For each window, the two cross covariances were calculated, and a linear slope was fit to the cross-covariance curves in the $lag = \pm 5$ region. Fig. 10 shows the cross-covariance slopes for each of these 45 second samples. The plot shows good feature separation for use in a linear classifier.

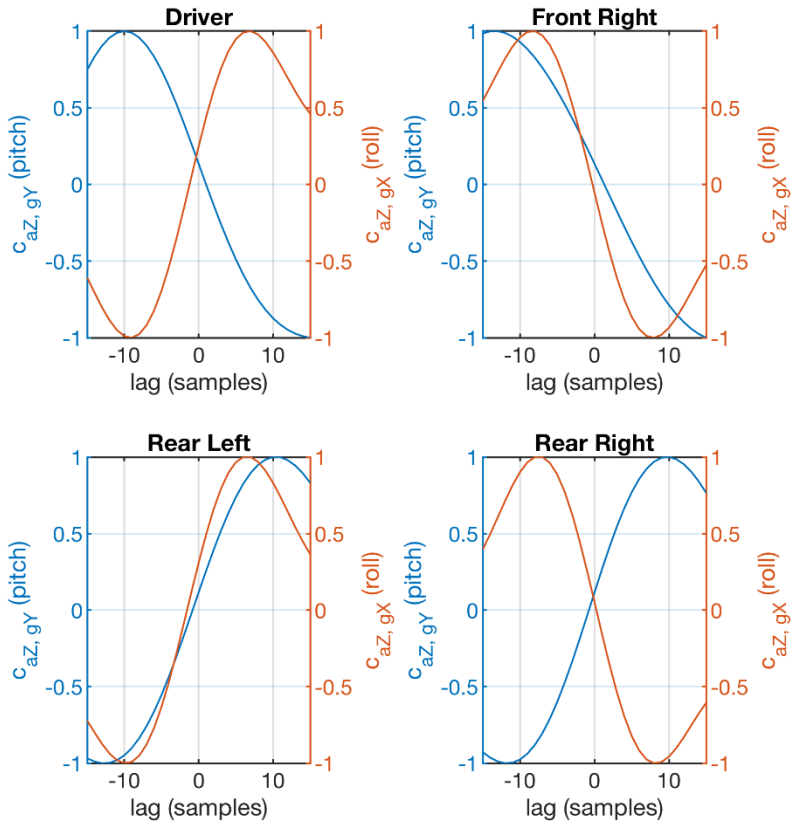

Fig. 9: Normalized cross covariances for experimental driving data. Each data set represents 5 minutes of driving. Blue curves are cross covariance of vertical acceleration and pitch-axis angular rate. Red curves are cross covariance of vertical acceleration and roll-axis angular rate. Each seat position has a clearly unique pattern of cross-covariances and its variation with time lag.

The above features were used as training inputs to a multi-class classifier made up of two binary support vector machines (SVM) [12]. The SVM fits the maximum margin hyperplane in the feature space (see Fig. 10) by maximizing the distance between the hyperplane and the nearest data points. In the case of a 2-dimensional feature space, the hyperplane is a line. The data here consisted of 77 labelled 45 second samples of driving data. The SVM was trained using all the data and validated using k-fold cross validation, which is preferred over a simple random separation of the data into single train and single test sets [13]. In k-fold cross validation, the 77

samples are randomly divided into k groups, or folds. One fold is held out, and the remaining k-1 folds are used to train an SVM. This process is then repeated a total of k times, such that each group gets used once as the test group. The overall accuracy of the SVM trained using all of the data is estimated by taking the mean accuracy of the k SVMs. Common choices for k are 5 and 10. As k gets larger, the computational cost increases, as more models must be trained, but the estimated performance approaches the true performance [13]. The limit for k is n, where n is the number of labelled data samples. In this case, the validation scheme is referred to as leave-one-out cross validation, as only one sample is held out to test, and n SVMs are trained.

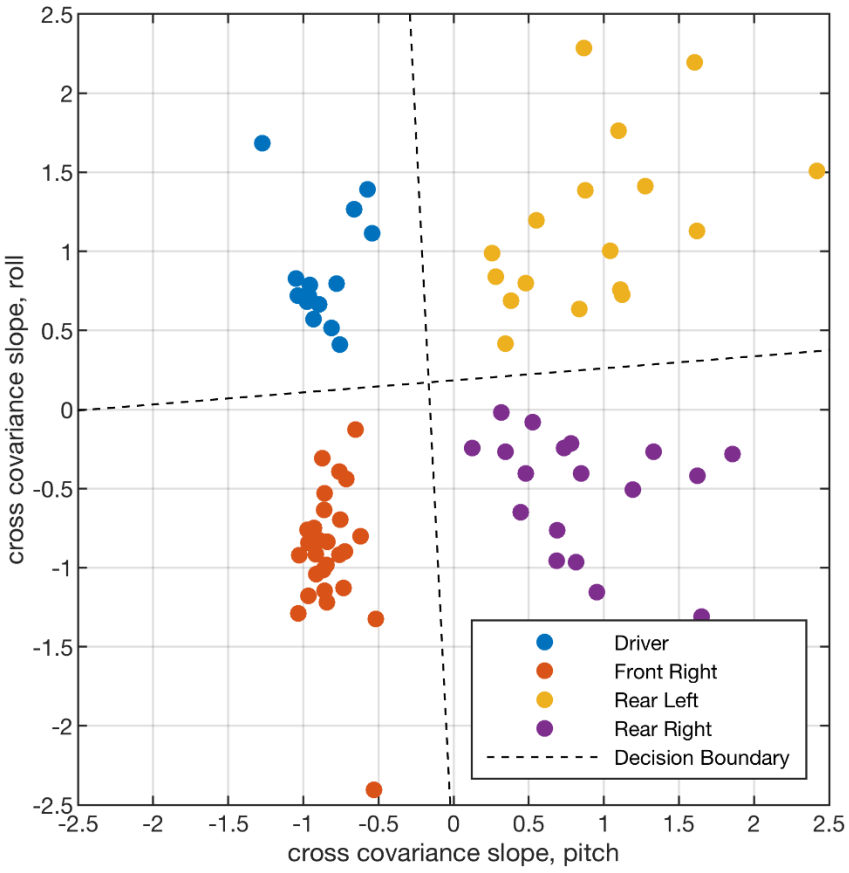

Fig. 10: Feature data used to train the SVM classifier. Data has been normalized to have zero mean and standard deviation of one. Each marker represents a 45-second-long experimental data set of city driving. The x-axis is the fitted slope of the cross covariance of vertical acceleration and pitch-axis

angular velocity. The y-axis is the fitted slope of the cross covariance of vertical acceleration and roll-axis angular velocity. The dashed lines represent the SVM decision boundaries.

Here, the accuracy of the classification for the vehicle experimental data was found to be 100% under both 5-fold and 10-fold cross validation, meaning that each binary SVM (left/right and front/rear) predicted the held-out fold with 100% accuracy for all 5 and 10 training rounds, respectively. Finally, experimental validation was also performed using leave-one-out cross validation, and the classification accuracy was again found to be 100% on all 77 folds. The dashed lines in Fig. 10 are the maximum margin hyperplanes for the two binary SVMs.

7. Conclusions

This paper presented a novel method for the localization of a smartphone inside a vehicle using the motion data gathered by the IMU in the phone. Unlike previous work, the method requires no external hardware, no wireless communication with the vehicle, and no access to the phone's camera. It only uses the sensors already available on the phone.

First, the orientation of the phone relative to the car is determined, which can be done without relying on the error-prone magnetometer. Based on the vehicle dynamics measured by the phone, it was shown that using the cross covariances of vertical acceleration to the pitch-axis angular velocity and vertical acceleration to the roll-axis angular velocity provides a viable classification feature for determining which seat the phone is in. A total of 40 minutes of driving data was collected and used to train two binary support vector machines to differentiate between front/rear and left/right seat positions. The support vector machines achieved 100% accuracy on the 40 minute data set, validated using 5-fold, 10-fold, and leave-one-out cross validation. The 100%

accuracy with experimental data shows that the developed system works extremely reliably.

Distracted driving due to phone usage is a major cause of vehicular accidents in the US, and there is a clear need for algorithms that can detect when a phone user is driving and automatically disable distracting features. Current phone apps are only able to detect whether the phone is in a moving car and then disable the use of texting during car motion. However, these apps are unable to detect whether the phone is being used by the driver or merely by a passenger of the car. The technology developed in this paper could thus be a very valuable tool for correctly disabling texting features only for the driver of the vehicle.

A limitation of the technology developed in this paper is that the orientation of the phone is assumed to be constant. If the orientation varies during use, then the developed signal processing algorithms will still work, but only if the change in orientation is slow, so that the orientation computation algorithm can recompute the lateral and longitudinal acceleration components correctly. It is also assumed that the terrain is flat. Significant road gradients can therefore result in errors.

Acknowledgments

This research was supported in part by a research grant from the National Science Foundation (NSF Grant PFI-1631133).

References

[1] *Injury Facts*. National Safety Council, 2015.

[2] E. O. Olsen, R. A. Shults, and D. K. Eaton, “Texting While Driving and Other Risky Motor Vehicle Behaviors Among US High School Students,” *Pediatrics*, vol. 131, no. 6, pp. e1708–e1715, 2013.

[3] Y. Wang, J. Yang, H. Liu, Y. Chen, M. Gruteser, and R. P. Martin, “Sensing Vehicle Dynamics for Determining Driver Phone Use,” in *Proceeding of the 11th Annual International Conference on Mobile Systems, Applications, and Services*, New York, NY, USA, 2013, pp. 41–54.

[4] Z. He, J. Cao, X. Liu, and S. Tang, “Who Sits Where? Infrastructure-Free In-Vehicle Cooperative Positioning via Smartphones,” in *Sensors*, 2014.

[5] J. Yang *et al.*, “Sensing Driver Phone Use with Acoustic Ranging through Car Speakers,” *IEEE Trans. Mob. Comput.*, vol. 11, no. 9, pp. 1426–1440, Sep. 2012.

[6] C. Bo *et al.*, “Detecting Driver’s Smartphone Usage via Nonintrusively Sensing Driving Dynamics,” *IEEE Internet Things J.*, vol. 4, no. 2, pp. 340–350, Apr. 2017.

[7] H. Chu, V. Raman, J. Shen, A. Kansal, V. Bahl, and R. R. Choudhury, “I am a smartphone and I know my user is driving,” in *2014 Sixth International Conference on Communication Systems and Networks (COMSNETS)*, 2014, pp. 1–8.

[8] J. G. Elias, *Driver handheld computing device lock-out*. 2014.

[9] R. Rajamani, *Vehicle dynamics and control*, 2nd ed.. New York: Springer, 2012.

[10] F. L. Markley, *Fundamentals of spacecraft attitude determination and control*. New York, NY: Springer, 2014.

[11] V. K. Ingle, *Digital signal processing using MATLAB*. Pacific Grove: Brooks/Cole, 2000.

[12] K. P. Bennett and C. Campbell, “Support Vector Machines: Hype or Hallelujah?,” *SIGKDD Explor.*, vol. 2, pp. 1–13, 2000.

[13] M. Kuhn, *Applied predictive modeling*. New York: Springer, 2013.

[14] T. Shim and C. Ghike, "Understanding the Limitations of Different Vehicle Models for Roll Dynamics Studies," *Vehicle System Dynamics*, Vol. 45, No. 3, pp. 191-216, 2007.

[15] V.T. Vu, O. Sename, L. Dugard and P. Gaspar, "Enhancing Roll Stability of Heavy Vehicle by LQR Active Anti-Roll Bar Control Using Electronic Servo-Valve Hydraulic Actuators," *Vehicle System Dynamics*, Vol. 55, No. 9, 2017.

[16] C.E. Beal and C. Boyd, "Coupled Lateral-Longitudinal Vehicle Dynamics and Control Design with Three-Dimensional State Portraits," *Vehicle System Dynamics*, in press, accepted 08 April, 2018, available online at https://doi.org/10.1080/00423114.2018.1467019.